Generation of synchronized femtosecond and picosecond laser pulses in a two-beam-pumped Ti:sapphire laser

Changjun Zhu (朱长军)[1*], Junfang He (贺俊芳)[2], Xuejun Zhai (翟学军)[1], Bing Xue (薛 兵)[1], and Chonghui Zhang (张崇辉)[1]

[1]*Department of Physics, School of Science, Xi'an Polytechnic University, Xi'an 710048, China*

[2]*State Key Laboratory of Transient Optics and Photonics, Xi'an Institute of Optics and Precision Mechanics, Chinese Academy of Sciences, Xi'an 710119, China*

[*]*E-mail: cjzhu@xpu.edu.cn*

Received April 14, 2009

Two operating modes, independent self-mode-locking and cross-mode-locking, are presented in a two-beam-pumped double-cavity dual-wavelength femtosecond Ti:sapphire laser. Synchronization of femtosecond and picosecond laser pulses is achieved by properly adjusting the cavity length matching and distributing the pump laser powers in the two laser cavities, and moreover, a timing jitter of 517 fs between femtosecond and picosecond pulses is obtained, with wavelength tuning ranges around 36 and 22 nm in the femtosecond and picosecond cavities, respectively.

OCIS codes: 140.4050, 140.7090.

doi: 10.3788/COL20100802.0194.

Synchronization of pump and probe optical pulses is of fundamental significance in a pump-probe scheme, which has been developed into an increasingly powerful technique in ultrafast laser spectroscopy and relevant inter disciplines. Synchronized femtosecond pulses generated from cross-mode-locked dual-wavelength femtosecond lasers, with extremely small timing jitter, have been extensively utilized in two-wavelength pump-probe schemes. In particular, synchronized femtosecond and picosecond pulses are of great interest in the observation of the oscillation periods of heavy-hole exciton density in a semiconductor quantum well[1], and two-color photoionization experiments[2].

Two categories of synchronization techniques, the active synchronization[3−6] and passive synchronization[7−15], have hitherto been employed to synchronize two femtosecond laser pulses. The active synchronization is fulfilled by precisely controlling the laser cavity length using complicated optoelectronic feedback systems. In contrast, the passive synchronization is achieved by nonlinear optical effects produced by two laser pulses in a shared laser medium. Recently, multi-pulse operation of a Kerr-lens mode-locked femtosecond laser has been accomplished[16]. Moreover, a tunable dual-wavelength Ti:sapphire laser system with quasi-continuous-wave and high-power outputs has been demonstrated, and an optical-to-optical conversion efficiency of 22.2% has been obtained[17].

So far, synchronized femtosecond and picosecond pulses has been generated in a one-beam-pumped dual-wavelength femtosecond Ti:sapphire laser[18]. Passively synchronized femtosecond pulses at 850 nm and picosecond pulses at 1064 nm have been obtained from two different laser cavities, Nd:YVO_4 laser cavity and Ti:sapphire one[19]. However, little effort has been devoted to synchronization of femtosecond and picosecond pulses in two-beam-pumped laser structures with a shared laser medium. In this letter, a two-beam-pumped resonant cavity structure is employed to allocate unequally the pump power in the two laser cavities, and a relatively higher intensity of the picosecond pulses, hence a more intense, cross-phase modulation (XPM), is obtained in the two-beam-pumped Ti:sapphire laser, subsequently, passively synchronized femtosecond and picosecond pulses are obtained, with a timing jitter of 517 fs.

The experimental schematics of the two-beam-pumped Ti:sapphire laser is presented in Fig. 1. A beam of Ar^+ laser of 10 W was split into two parallel beams, with powers of 6.5 and 3.5 W, respectively. The two beams were focused by a 100-mm focal-length lens into a 4-mm-long Ti:sapphire (Ti:S) crystal. The radii of M_1 and M_2 are 100 mm. M_1, M_2, M_3, and M_4 are reflectors with high veflectivities from 700 to 900 nm. M_5 is a chirped mirror, and M_6 and M_7 are output couplers of 3% transmission. P_1 and P_2 are quartz prisms, which are separated by 56 cm for the second-order dispersion compensation. The femtosecond cavity, pumped by a power of 3.5 W, is composed of M_3, P_1, P_2, M_1, M_2, and M_6. The picosecond cavity, pumped by a power of 6.5 W, consists of M_5, M_4, M_1, M_2, and M_7. The temporal widths of the femtosecond laser pulses were measured by a second-order interferometric autocorrelation with an actively stabilized Michelson interferometer, the temporal widths of the picosecond laser pulses were measured by a second-order intensity autocorrelation, and the crosscorrelation was measured by sum-frequency of the two laser pulses in a BBO crystal. The laser

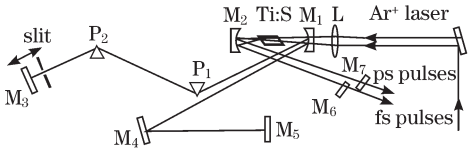

Fig. 1. Schematic arrangement of the two-beam-pumped double-cavity dual-wavelength femtosecond Ti:sapphire laser.

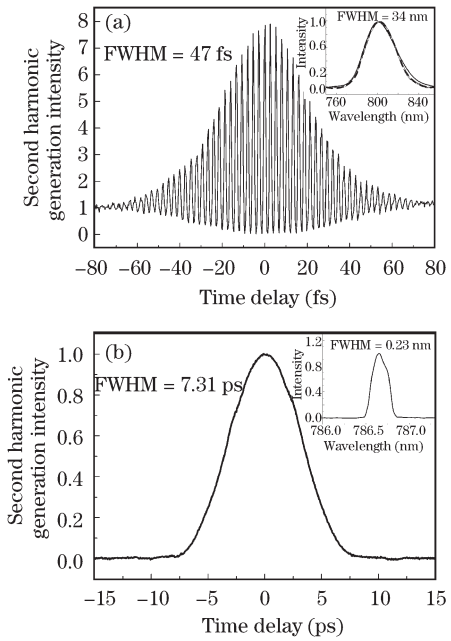

Fig. 2. Independent self-mode-locking. (a) The second-order interferometric autocorrelation and spectrum (inset) of the pulses in the femtosecond cavity. (b) The second-order intensity autocorrelation and spectrum (inset) of the pulses in the picosecond cavity.

spectrum was recorded by a spectrometer.

The two laser cavities were able to operate simultaneously in independent self-mode-locking modes. Figure 2(a) shows the interferometric autocorrelation of the pulses generated from the independent self-mode-locked femtosecond cavity, with the measured spectrum (dashed line) and the Fourier transform spectrum (solid line) presented in the inset. Compressed with a pair of prisms outside the cavity, the femtosecond pulses exhibit high quality. The envelope of the interferometric autocorrelation width measured as full-width at half-maximum(FWHM) is 47 fs, and the wavelength is centered at 801 nm, with a spectral width of 34 nm (FWHM). Gaussian pulse is assumed, the femtosecond pulse width is 0.707×47 fs = 33 fs, and the spectral width is 34 nm, which is corresponding to 15.9 THz, giving rise to a time-bandwidth product of 0.52, which is close to the time-bandwidth product of a Gaussian pulse, 0.441. Figure 2 (b) shows the intensity autocorrelation and the spectrum of the pulses generated from the independent self-mode-locked picosecond cavity. The intensity autocorrelation width is 7.31 ps and the wavelength is centered at 786.7 nm, with a spectral width of 0.23 nm. The difference between the measured spectrum and the Fourier transform spectrum is due to the fact that the Fourier transform spectrum possesses a low resolution determined by the limited time delay scan range of the autocorrelation measurement. Difference in the pulse widths in the two cavities is attributed to different group velocity dispersion (GVD) compensations and different self-phase modulation (SPM) in the two cavities.

It is of interest to note that the laser system was able to operate in cross-mode-locking mode. Towards this end, independent self-mode-locking in each cavity was first achieved simultaneously in the two cavities, and then, the femtosecond cavity length was adjusted to match the picosecond cavity length. In the meantime, a frequency counter was implemented to monitor the repetition rates of the pulses in the two cavities. The coupling occurred within a cavity length mismatch of about 0.3 μm and the wavelength shifts were 1 and 5 nm for femtosecond and picosecond pulses, respectively. When the lengths of the two laser cavities were matched, XPM-induced cross-mode-locking occurred in the laser medium, which was indicated by an identical pulse repetition rate for both cavities and leaded to remarkable variations of the pulse properties.

Figure 3(a) shows the interferometric autocorrelation of the pulses in the cross mode-locked femtosecond cavity, with the measured spectrum (dashed line) and the Fourier transform spectrum (solid line) displayed in the inset. The interferometric autocorrelation envelope width is 53 fs and the spectral width is 33 nm, centered at 800 nm. Figure 3(b) shows the intensity autocorrelation and the spectrum of the pulses in the cross-mode-locked picosecond cavity. The intensity autocorrelation width is 1.26 ps and the spectral width is 1.24 nm, centered at 781.3 nm.

A close comparison of Figs. 2 with 3 reveals that the picosecond pulse width shortens noticeably and the spectrum broadens considerably. In the femtosecond cavity, however, the pulse width and the spectrum remain almost invariant. The above observation is interpreted in terms of the XPM-induced variation. Moreover, in the cross-mode-locking regime, the central wavelength shift of the picosecond pulse is found to be highly sensitive to the cavity length mismatch. The sensitive dependence of the XPM-induced wavelength shift on cavity length

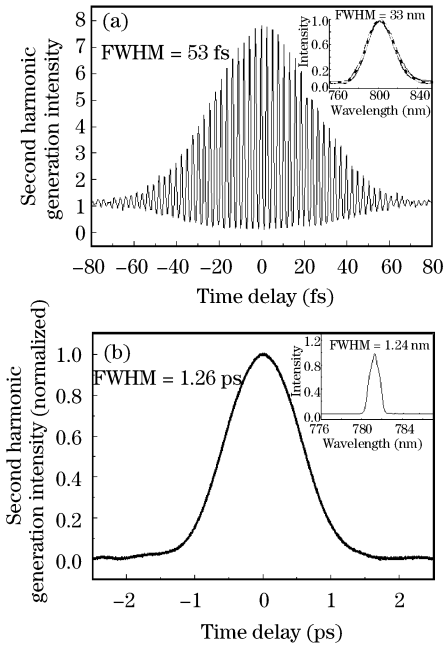

Fig. 3. Cross-mode-locking. (a) The second-order interferometric autocorrelation and spectrum (inset, dashed line: measured spectrum, solid line: Fourier transform spectrum) of the pulses in the femtosecond cavity. (b) The second-order intensity autocorrelation and spectrum (inset) of the pulses in the picosecond cavity.

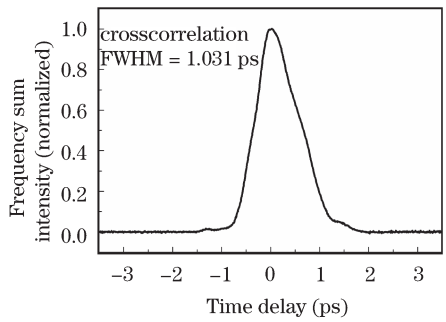

Fig. 4. Intensity crosscorrelation for cross-mode-locking.

mismatch was observed previously as well[11]. Numerical simulations disclose that the XPM-induced wavelength shift is not only sensitive to the time delay, but also to the interaction length in the laser crystal[13,20]. Additionally, the cross-mode-locking is sensitive to the change of the ratio of one pump power to the other. The sensitivity of the operating output power, however, is not very sensitive to the pump powers.

Timing jitter between two pulses determines, to a considerable extent, the time resolution of pump-probe devices in which the two pulses are employed as pump and probe pulses. Crosscorrelation was utilized to measure the timing jitter between the femtosecond and picosecond laser pulses, and the result is shown in Fig. 4. Since the laser pulses are closed to Gaussian pulses, as stated previously, we can calculate the timing jitter by Gaussian pulse approximation, which is

$$T_j = [t^2 - (t_1^2 + t_2^2)]^{\frac{1}{2}}, \tag{1}$$

where t is the crosscorrelation width, t_1 is one of the pulse width, and t_2 is the other pulse width. Under Gaussian pulse approximation, $t = 1.031$ ps, $t_1 = 0.053 \times 0.707 = 0.0375$ ps, and $t_2 = 1.26 \times 0.707 = 0.891$ ps, which are giving rise to a timing jitter of 517 fs.

Operating in the cross-mode-locking mode, inasmuch as the femtosecond and picosecond pulses interact mutually in the laser medium, the femtosecond and picosecond cavities can concurrently be tuned by adjusting the prisms and slit position. The maximum wavelength tuning ranges in the femtosecond and picosecond cavities are 36 and 22 nm, respectively.

In conclusion, two operating modes, independent self-mode-locking, and cross-mode-locking have been demonstrated in a two-beam-pumped double-cavity dual-wavelength femtosecond Ti:sapphire laser. In the independent self-mode-locking mode, the mode-locking mechanism for both the femtosecond and picosecond cavities is the self-mode-locking governed by GVD and SPM. As a contrast, in the cross-mode-locking mode, the mode-locking mechanism is cross-mode-locking induced by XPM. The timing jitter of 517 fs between the femtosecond and picosecond pulses, and the large wavelength tuning ranges of the femtosecond and picosecond pulses broaden the applications of the laser in ultrafast laser spectroscopy.

This work was supported by the Natural Science Foundation of Shaanxi Province of China (No. 2007A23), the Special Scientific Research Project Foundation of the Education Department of Shaanxi Province of China (No. 08JK295), and the National Natural Science Foundation of China (No. 10576037).

References

1. A. Schüelzgen, R. Binder, M. E. Donovan, M. Lindberg, K. Wundke, H. M. Gibbs, G. Khitrova, and N. Peyghambarian, Phys. Rev. Lett. **82,** 2346 (1999).
2. M. Meyer, D. Cubaynes, P. O. Keeffe, H. Luna, P. Yeates, E. T. Kennedy, J. T. Costello, P. Orr, R. Taïeb, A. Maquet, S. Düsterer, P. Radcliffe, H. Redlin, A. Azima, E. Plönjes, and J. Feldhaus, Phys. Rev. A **74,** 011401 (2006).
3. L. S. Ma, R. K. Shelton, H. C. Kapteyn, M. M. Murnane, and J. Ye, Phys. Rev. A **64,** 021802 (2001).
4. Z. Y. Wei, Y. Kobayashi, Z. G. Zhang, and K. Torizuka, Opt. Lett. **26,** 1806 (2001).
5. R. K. Shelton, S. M. Foreman, L. S. Ma, J. L. Hall, H. C. Kapteyn, M. M. Murnane, M. Notcutt, and J. Ye, Opt. Lett. **27,** 312 (2002).
6. A. Bartels, S. A. Diddams, T. M. Ramond, and L. Hollberg, Opt. Lett. **28,** 663 (2003).
7. M. R. X. de Barros and P. C. Becker, Opt. Lett. **18,** 631 (1993).
8. D. R. Dykaar and S. B. Darack, Opt. Lett. **18,** 634 (1993).
9. J. M. Evans, D. E. Spence, D. Burns, and W. Sibbett, Opt. Lett. **18,** 1074 (1993).
10. Z. G. Zhang and T. Yagi, Opt. Lett. **18,** 2126 (1993).
11. A. Leitenstorfer, C. Fürst, and A. Laubereau, Opt. Lett. **20,** 916 (1995).
12. M. Betz, F. Sotier, F. Tauser, S. Trumm, A. Laubereau, and A. Leitenstorfer, Opt. Lett. **29**, 629 (2004).
13. S. C. Wang, C. J. Zhu, J. F. He, H. R. Yang, D. Xiao, X. Hou, Appl. Phys. B **69**, 211 (1999).
14. J. R. Tian, Z. Y. Wei, P. Wang, H. H. Han, J. Zhang, L. H. Zhao, Z. H. Wang, J. Zhang, T. Yang, and J. W. Pan, Opt. Lett. **30,** 2161 (2005).
15. P. Zhou, Z. Chen, X. Wang, X. Li, Z. Liu, X. Xu, J. Hou, and Z. Jiang, Chin. Opt. Lett. **6,** 523 (2008).
16. J. Wu, H. Cai, X. Han, and H. Zeng, Chin. Opt. Lett. **6,** 76 (2008).
17. X. Ding, M. Pang, X. Y. Yu, X. H. Wang, S. M. Zhang, H. Zhang, R. Wang, W. Q. Wen, P. Wang, and J. Q. Yao, Chin. Phys. Lett. **24,** 1938 (2007).
18. C. J. Zhu, J. F. He, and S. C. Wang, Opt. Lett. **30,** 561 (2005).
19. W. Seitz, T. R. Schibli, U. Morgner, F. X. Kärtner, C. H. Lange, W. Richter, and B. Braun, Opt. Lett. **27,** 454 (2002).
20. P. L. Baldeck, R. R. Alfano, and G. P. Agrawal, Appl. Phys. Lett. **52,** 1939 (1988).